Volume 18, No 3 | International Journal of Radiation Research, July 2020

Development of radiolabeled dextran coated iron oxide nanoparticles with ^{111}In and its biodistribution studies

S.H. Mousavie Anijdan[1], A. Gholami[2], A. Lahooti[3*]

[1]*Department of Medical Physics, Babol University of Medical Sciences, Babol, Iran*
[2]*Department of Nuclear Medicine, Shahid Beheshti Hospital, Babol University of Medical Sciences, Babol, Iran*
[3]*Department of Medical Physics and Biomedical Engineering, School of Medicine, Tehran University of Medical sciences, Tehran, Iran*

► ***Original article***

***Corresponding authors:**
Afsaneh Lahooti, Ph.D.,
E-mail:
lahootia@razi.tums.ac.ir

Revised: June 2019
Accepted: August 2019
Int. J. Radiat. Res., July 2020; 18(3): 539-547
DOI: 10.18869/acadpub.ijrr.18.3.539

ABSTRACT

Background: The main aim of this study is to radiolabel dextran coated iron oxide nanoparticles (NPs) (with 80 nm hydrodynamic size) with the Indium-111 and evaluation their biodistribution after intravenous injection normal mice. ***Materials and Method:*** The chelator Diethylenetriamine Pentaacetic Acid (DTPA) dianhydride was conjugated to SPION using a small modification of the well-known cyclic anhydride method at a ratio of 1:5 (NPs:DTPA) molar ratio. The reaction was purified with magnetic assorting columns (MACs) using high gradient magnetic field following incubation. Then the radiochemical purity of the radiolabeled NPs were determined using RTLC method. The magnetic properties of nanoparticles were measured by a 1.5 tesla clinical human MRI. ***Results:*** The NPs showed high super paramagnetic properties whereas their r_2/r_1 was 17.6. The RTLC showed that the purity of compound was above 99% after purification and the compound has shown a good in-vitro stability until 6 hours in the presence of human serum. The biodistribution of ^{111}In-DTPA-NPs in mice demonstrated high uptake in the reticuloendothelial system (RES) and the blood clearance was so fast. ***Conclusion:*** Due to magnificent uptakes of this radiotracer in the liver and spleen, its stability and their fast clearance from other tissues, especially in blood, it is suggested that this radiotracer would be suitable for RES theranostics purposes.

Keywords: *Dextran-coated superparamagnetic iron oxide, ^{111}In radioisotope, biodistribution, theranostics, reticuloendothelial system, radiopharmaceuticals.*

INTRODUCTION

Iron oxide nanoparticles (NPs) are capable to reduce the signal intensity in T_2 or T_2*-weighted images among other types of magnetic resonance imaging (MRI) contrast agents [1, 2]. These NPs have flexible uses in different medical fields such as imaging [2], lymph node detection [3], drug delivery [4], therapy [5] and cell tracking [6]. The iron oxides NPs are used as negative contrast agents in MRI and depending on their sizes called as USPIOs (ultra-superparamagnetic iron oxide) or SPIOs (Super paramagnetic iron oxide) [7]. Dextran-coated nanoparticles maintained in the liver up to several days post injection and they are suitable carriers with high potential for liver and spleen therapies. Recent studies are focused on the manipulating of these nanoparticles as dual modalities contrast agents for positron emission tomography (PET) combined with MRI or PET/MRI or in can be used in single photon emission computed tomography (SPECT) combined with MRI or SPECT/MRI [8]. According to our previous studies, we suggested that these labeled nanoparticles NPs could be suitable to be used

[Downloaded from ijrr.com on 2025-07-12]
[DOI: 10.18869/acadpub.ijrr.18.3.511]

as diagnostic agents for spleen and liver malignancies.

Among all of the radioisotopes used in nuclear medicine, Indium-111 is a radionuclide with physical half-life of 2.8047 days which emits gamma rays with energies of 171.28 keV (90%) and 245.40 keV (94%) [9]. In addition, it emits 8 Auger electrons and a beta radiation with 448.28(100%) [10]. The interesting physical and chemical properties and availability of Indium-111 make it an interesting nuclide for radiopharmaceutical research [11].

In this study, we try to develop ^{111}In-DTPA-SPION as a theranostics radiotracer, which can be applied as dual contrast agents in MRI and SPECT imaging.

MATERIALS AND METHODS

Nanomag®-CLD-SPION NPs were provided from Micromod (Micromod Partikel technologie GmbH) with 80 nm hydrodynamic size. These nanoparticles were cross linked dextran-coated iron oxide particles with NH_2 functional group on their surface. The iron concentration of the nanoparticles was 2.4 mg/mL. Production of [^{111}In] was performed at the Agricultural, Medical and Industrial Research School (AMIRS), 30 MeV cyclotron (Cyclone-30, IBA, Louvain-la-Neuve, Belgium) using ^{112}Cd (p, 2n) ^{111}In reaction. Enriched cadmium sulfate with a purity of >99% was obtained from American elements Co. USA. Calculations were based on the 171.28 keV peak for ^{111}In [12]. Radiochemical purity of the radiolabeled NPs were determined RTLC using Whatman paper and Bioscan AR2000 (from Paris, France) scanner. Whatman No.2 paper was obtained from Whatman (Maidstone, UK). All other chemical reagents were purchased from Sigma-Aldrich Chemical Co. U.K. A high-purity germanium (HPGe) detector, coupled with a Canberra™ multichannel analyzer (model GC1020-7500SL, Canberra Industries Inc., CT, U.S.A.) and a dose calibrator ISOMED 1010 (Elimpex-Medizintechnik, Austria) was used for measuring the mice organ activities. All values were expressed as mean ± standard deviation (Mean ± SD). Moreover, animal studies were performed in accordance with the Laboratory Animal Care (NIH publication) [13].

Particles Characterizations

The particle core size and structure of the SPIONs were checked with a TEM (transmission electron microscope, PHILIPS, CM 30). Photon correlation spectroscopy (PCS) was used to determine the hydrodynamic diameter of the particle samples. These measurements were performed with a Malvern Zeta sizer Nano ZS-90 (Malvern Instruments Ltd., Worcestershire, UK). Finally, Iron concentration of suspensions was acquired with inductively coupled plasma atomic emission spectroscopy (ICP-AES, Varian-Liberty, 150 AX Turbo, USA) of digested samples with boiling HNO_3 [14].

Magnetic resonance imaging

Magnetic resonance imaging of different dextran-coated SPIOs was performed at 20 ˚C using 1.5T (Magnetom Avanto; Siemens, Erlangen, Germany) MR scanners. Various concentrations of each sample (0.2, 0.1, 0.05, 0.025 and 0.0125 mg Fe/mL) were prepared and placed in the plastic container, filled with water in order to avoid susceptibility artifacts of surrounding air and impounded for one hour to equilibrate temperature [15].

Then images transferred to a local workstation in order to be analyzed quantitatively and the T_1 and T_2 maps were calculated assuming mono-exponential signal decay. T_1 measurements (longitudinal relaxation) were done using SE sequences with fixed TE of 12 ms and variable TRs that saves acquisition time in order to reach higher temperature stability in comparison to variable Inversion time (TI) method. A non-linear function least-square curve fitting on a pixel-by-pixel basis were applied to calculate T_1 value with the TR values of 150, 300, 500, 1000, 2000, 3000, and 5000 ms. For T_1 maps, the signal intensity of each pixel expressed as equation (1):

$$SI_{(\text{pixel i,j})} = S_{0(pixel\,i,j)}\left[1 - e^{-TR/T1_{(\text{pixel i,j})}}\right] \quad (1)$$

[Downloaded from ijrr.com on 2025-07-12]

[DOI: 10.18869/acadpub.ijrr.18.3.511]

Five SE images with fixed TR value of 3000 ms and TE values of 12, 24, 36, 48 and 60 ms were obtained, in order to calculate T_2 maps and signal intensity of each pixel expressed according to equation (2):

$$SI_{(\text{pixel } i,j)} = S_{0(pixel\, i,j)} \left[e^{-TE/T2_{(\text{pixel } i,j)}} \right] \quad (2)$$

Care was taken to exclude signal intensities not significantly above the noise level and calculated regression coefficient determined as curve fit quality [16].

Radiolabeling of SPION with ^{111}In

Conjugation of NPs with cyclic DTPA di-anhydride

The chelator DTPA di-anhydride was conjugated to NPs using a small modification of the well-known cyclic anhydride method [17, 18]. Conjugation was performed at a molar ratio of 1:5 (SPION:DTPA) molar ratio. In brief, 1 mg of NPs (4.3 μM) and 2.10 mg DTPA anhydride (13.76 μM) were mixed in 0.3 mL of 0.1 M phosphate buffer solution (pH = 7.0) and 0.3 mL of normal saline and stirred at room temperature (RT) under N_2 for 30 minutes [19].

Radiolabeling of the conjugated SPIONs

The SPIONs was labeled with ^{111}In using an optimized protocol according to the literature [20]. Typically, 102-105 MBq of ^{111}In-chloride (in 0.2M HCl) was added to a conical vial and dried under a flow of nitrogen. The conjugated fraction was added to the ^{111}In containing vial, in 1 mL of phosphate buffer (0.1 M, pH 6.5) and mixed gently for 2 minutes. The resulting solution was incubated at room temperature (RT) for 45 minutes. Following incubation, the radio labeled conjugate was checked using RTLC method for labeling and purity checked. The complex reaction was purified with magnetic assorting columns (MACs) (Miltenyi Biotec) using high gradient magnetic field [21].

Purification of ^{111}In-DTPA-SPIONs

In order to purify the final solution, it was run through a strong stationary magnetic field using MACs columns in order to trap the iron oxide NPs in the magnetic column. All the magnetic materials (included labeled and non-labeled SPIONs) were trapped via a MACS column. The column was washed 3 times with PBS, while the column attached to high gradient magnet (MACS® Separation Unit, Miltenyi Biotec Inc, Germany), and after separating the column, the trapped NPs were washed with the 1 mL of PBS [21].

Quality control of ^{111}In-DTPA-SPIONs

Radiochemical purity were evaluated with a 1μL sample of the ^{111}In-DTPA-SPION complex that spotted on a Whatman No.2 chromatography paper, and performed in a 5mM DTPA as the mobile phase. The Rf values of free ^{111}In and ^{111}In-DTPA-SPION complex were 0.9 and 0.0, respectively. Labeling efficiency was calculated using the following equation (3) [22].

$$efficiency\ of\ radiolabeling\% = \frac{Total\ Counts - counts\ of\ free\ ^{111}In}{Total\ Counts} * 100 \quad (3)$$

Stability testing of the radio labeled compound in presence of human serum

For serum stability studies, 7 mL of blood is centrifuged at 3500 rpm for 5 minutes and then 1 mL of serum is withdrawn. 100 μL of the ^{111}In-DTPA-SPIONs was added to 1 mL of human serum and incubated at 37°C up to 24 hours. Aliquots of the reaction mixture were diluted 1:10 with PBS (pH 7.4) and analyzed by RTLC like the procedure described above at 1, 2 and 6 hours [23].

Biodistribution of ^{111}In-DTPA-SPION in normal mice

To determine its biodistribution, NPs was administered to normal Balb/c mice purchased from Razi Institute (Karaj, Iran). A volume (15μL) of the final ^{111}In-DTPA-SPION solution containing an activity of 2.7-3.7 MBq was injected intravenously to mice's tail veins. Four mice were sacrificed at specific time intervals (1, 5, 15, 30, 60 minutes and 2, 6, 24 and 48 hours post injections). After that, the specific activity was calculated for 17 various organs as a percentage of the injected dose per gram tissue (ID/g %) (Based on the area under the 171.28

[Downloaded from ijrr.com on 2025-07-12]

[DOI: 10.18869/acadpub.ijrr.18.3.511]

keV peak obtained by an HPGe detector) [12]. For each of these measurements, three samples (form each organ) were weighed and then counted by HPGe to determine the percentage of injected dose per gram (which was equivalent to the percentage of injected activity per gram % IA/g≡%ID/g) [24]; all the organ activity measurements were normalized to injected activity [25].

Measurement of activity

The activity in the syringes was measured before and after administration of the radiopharmaceutical with well-type ionization chamber (CRC-15R, Capintec, USA N.J.). All samples were background subtracted, the decay correction was performed, and then similar samples were averaged together. Uncertainties in the determinations were minimal, because each assay collected at least 10,000 counts, which results the standard deviation (SD) of less than 1% [26]. In all measurements, we try to keep same geometry and same volume in order to prevent overestimation and underestimation in dose measurements. All samples were background subtracted and decay correction was considered for all measurements. The similar samples were averaged together [27, 28].

The HPGe detector gave us counts, therefore we have used the equation (4) to convert the counts into the activity:

$$A(Bq)_{Tissue} = \frac{Area\ Under\ Curve}{t * Eff * Br} \quad (4)$$

Where t is the time of counts and Eff is the efficiency of the detector for the selected energy and Br is the decay yield of selected energy (171.28 keV) for the ^{111}In [11].

The ^{111}In activity concentration at time t, % ID/g (t), was then calculated as the percentage of injected activity per gram of tissue (%IA/g) [29] by suse of equation (5):

$$\%ID/g = \frac{A_{Tissue}/M_{Tissue}}{A_{Total}} * 100 \quad (5)$$

Where A_{tissue} represented as the ^{111}In activity in the sample, while M_{tissue} is the mass of the sample and A_{total} is the total activity of ^{111}In injected into the mouse.

Statistical analysis

Data have been represented as the mean of four individual observations with standard error of mean. Significance has been calculated using Student's *t*-test.

RESULTS

Figure 1 shows size information of the prepared SPIONs. As demonstrated in figure 1, the core size distribution of the NPs is narrow. The PCS histogram of SPIONs indicating their hydrodynamic magnitudes of about 80.23 nm.

The relaxation time of the NPs were represented in figure 2. The longitudinal and transverse relaxivities were obtained by calculating the slope of the graphs depicted in figure 2. As represented in figure 2, the r_2 of NPs was 308.00 ($mL*msec^{-1}*mg^{-1}$) whereas the r_1 value was 17.48 ($mL*msec^{-1}*mg^{-1}$) the R^2 values represented the goodness of fitting.

Figure 3 shown that the radionuclide purity of ^{111}In-DTPA-SPION was about 62% post labeling but after passing through the MACs column, it increased to 99%.

The results of stability of final product were depicted in figure 4. The labeling stability in presence of PBS and human serum were more than 93% and 86%, respectively after 6 hours in the RT.

The accumulation of ^{111}In-DTPA-SPION in the various organs are shown in Table 1. The results showed that most of the activity was accumulated in the reticuloendothelial system which known as RES (liver and spleen). Nearly all excretion of activity occurred by the renal system, and hepatobiliary excretion was insignificant. In order to better clarification of the liver and spleen and blood, we depicted them in figure 5.

[Downloaded from ijrr.com on 2025-07-12]

[DOI: 10.18869/acadpub.ijrr.18.3.511]

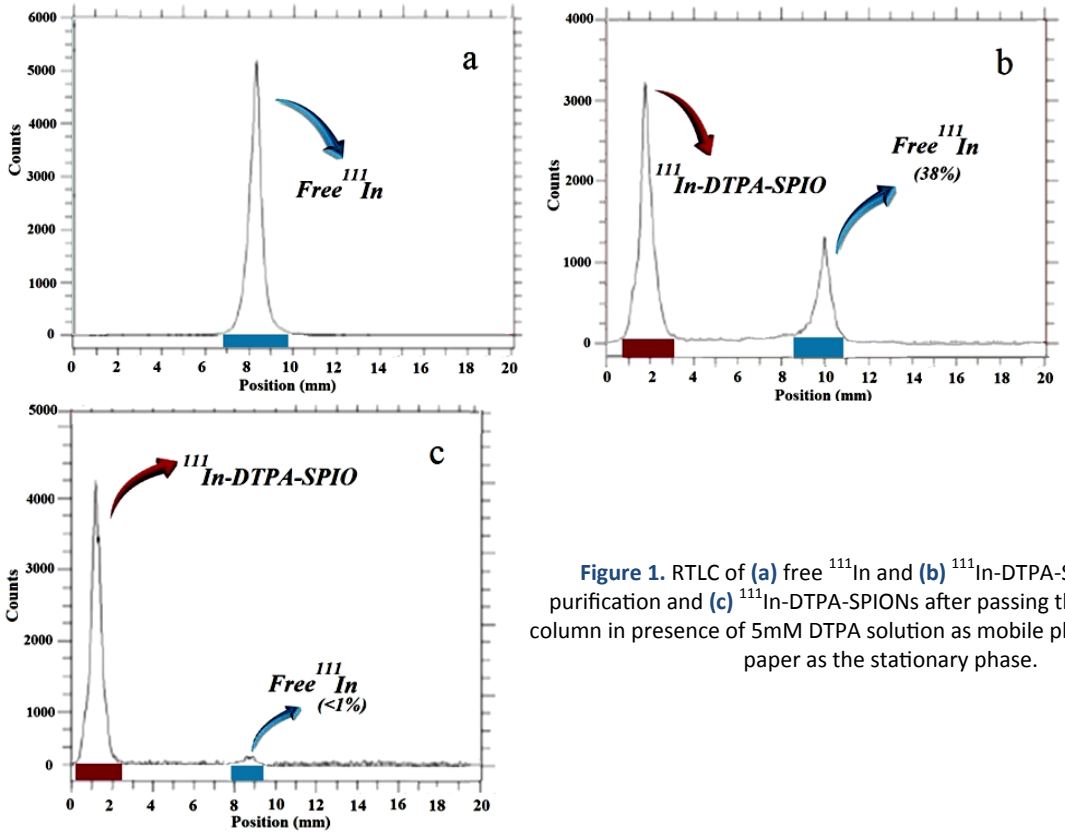

Figure 1. RTLC of **(a)** free ^{111}In and **(b)** ^{111}In-DTPA-SPIONs before purification and **(c)** ^{111}In-DTPA-SPIONs after passing through the MACs column in presence of 5mM DTPA solution as mobile phase and Whatman paper as the stationary phase.

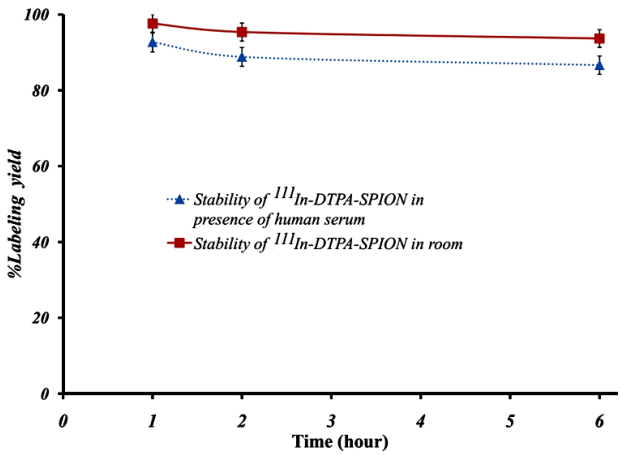

Figure 2. RTLC of ^{111}In-DTPA-SPION at different time points, in presence of human serum (dotted line) and in room temperature (the red line) in 5mM DTPA as mobile phase and Whatman paper as the stationary phase.

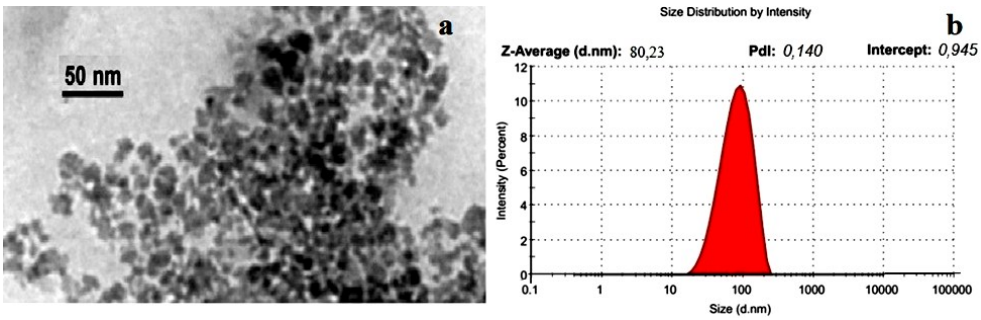

Figure 3. a: TEM of a SPIONs shows that the crystal core size of the particles is about 10.4±1.98 nm similar to our previous study and **b:** The PCS histogram of SPIONs indicating their hydrodynamic magnitudes of about 80.23 nm.

[Downloaded from ijrr.com on 2025-07-12]

[DOI: 10.18869/acadpub.ijrr.18.3.511]

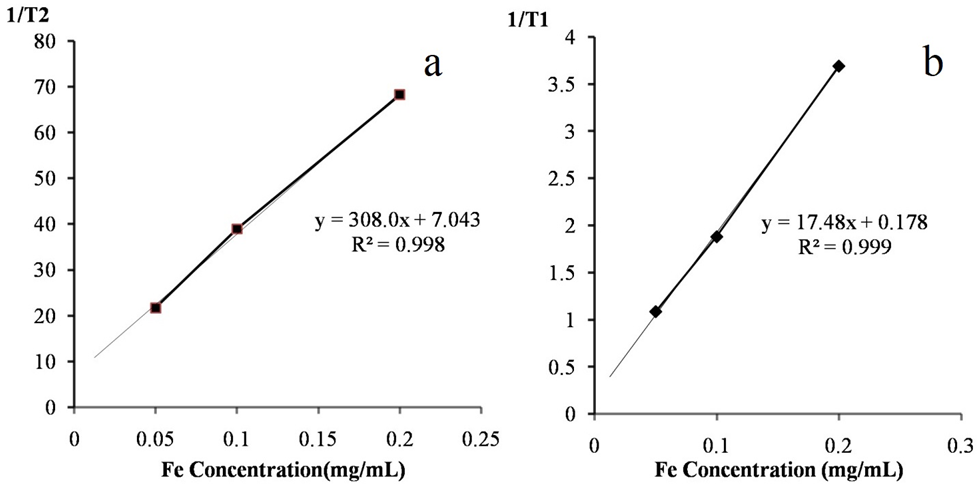

Figure 4. Plot of $1/T_2$ **(a)** and $1/T_1$ **(b)** versus Fe concentration (mg/mL). The slope of the line represents the longitudinal (r_1) and transverse (r_2) relaxivity.

Table 1. Biodistribution of 111In-DTPA-SPION in various time points (represented as injected dose per gram).

Tissues	1	5	Time				360	1440	2880
			15	30	60	120			
Blood	52.6±1.5	10.8±1.4	2.4±0.8	1.1±0.1	0.3±0.0	0.1±0.0	0.1±0.0	0.0±0.0	0.0±0.0
Intestine	0.2±0.0	0.2±0.0	0.3±0.1	0.3±0.1	0.2±0.0	0.1±0.0	0.0±0.0	0.0±0.0	0.0±0.0
Stomach	0.1±0.0	0.4±0.1	0.5±0.2	0.2±0.1	0.2±0.1	0.1±0.0	0.0±0.0	0.0±0.0	0.0±0.0
Muscle	0.1±0.0	0.2±0.0	0.1±0.0	0.1±0.0	0.1±0.0	0.0±0.0	0.0±0.0	0.0±0.0	0.0±0.0
Brain	0.0±0.0	0.0±0.0	0.0±0.0	0.0±0.0	0.0±0.0	0.0±0.0	0.0±0.0	0.0±0.0	0.0±0.0
Liver	24.5±1.7	49.5±3.1	63.3±2.7	69.8±3.7	66.9±2.9	63.2±2.2	55.2±1.9	40.7±1.2	31.8±1.4
Spleen	4.3±0.3	17.2±1.0	18.3±1.1	21.3±1.4	18.5±1.1	14.0±0.7	8.8±0.4	5.6±0.2	3.7±0.2
Heart	2.7±0.2	1.4±0.1	1.0±0.1	0.4±0.0	0.1±0.0	0.1±0.0	0.1±0.0	0.0±0.0	0.0±0.0
Kidney	4.2±0.3	5.5±0.7	3.7±0.3	2.2±0.2	1.3±0.1	1.2±0.0	0.8±0.0	0.2±0.0	0.0±0.0
Pancreas	1.3±0.1	0.5±0.1	0.4±0.0	0.3±0.0	0.2±0.0	0.1±0.0	0.1±0.0	0.0±0.0	0.0±0.0
Lung	5.5±0.3	2.8±0.3	1.8±0.1	1.4±0.1	1.2±0.3	0.8±0.0	0.4±0.0	0.0±0.0	0.0±0.0
Femur	0.4±0.0	0.5±0.1	0.4±0.0	0.3±0.0	0.3±0.0	0.3±0.0	0.1±0.0	0.1±0.0	0.0±0.0
Skin	0.2±0.0	0.1±0.0	0.1±0.0	0.1±0.0	0.0±0.0	0.0±0.0	0.0±0.0	0.0±0.0	0.0±0.0
Feces	0.0±0.0	0.0±0.0	0.1±0.0	0.2±0.0	0.4±0.1	0.7±0.1	1.3±0.1	2.4±0.2	2.6±0.1
Urine	0.0±0.0	0.1±0.0	1.7±0.1	2.4±0.1	4.0±0.2	3.7±0.2	3.3±0.1	2.2±0.1	1.3±0.1
Cascade	3.0±0.2	1.9±0.1	1.1±0.1	0.7±0.1	0.3±0.0	0.2±0.0	0.2±0.0	0.1±0.0	1.3±0.0

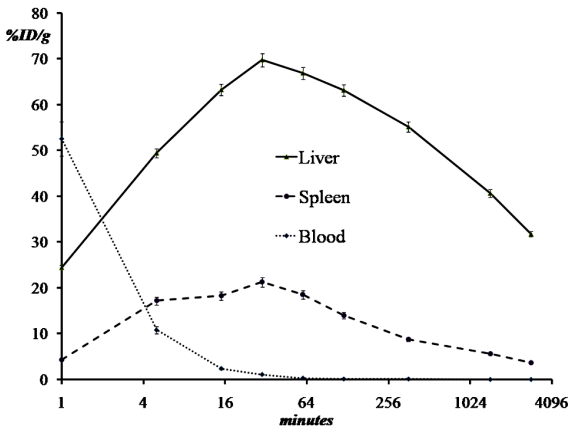

Figure 5. Clearance curve of the liver, spleen and blood in mice after intravenous injection the horizontal axis is expressed in logarithmic scale based 2.

[Downloaded from ijrr.com on 2025-07-12]

[DOI: 10.18869/acadpub.ijrr.18.3.511]

DISCUSSION

The labeling process of SPION-DTPA and purification of final product took about 1 hour. As demonstrated in figure 1, the purity of compound after purification was increased by 37% from 62% into almost %100. This high purified compound is due to the physics behind the MACs column which let the non-magnetic materials such as ^{111}In go down and grab the magnetic compounds such as DTPA-SPION and ^{111}In-DTPA-SPION while attaching to the magnet. The final product had a good stability as shown in figure 2 after 6 hours post labeling. The labeling stability in presence of PBS and human serum were more than 93% and 86%, respectively after 6 hours in the RT. The hydrodynamic size examination of the NPs showed that the size was not significantly changed after labeling. The size and the kinetic of the labeled NPs were in accordance to our previous studies. Compare to previous study carried out by Gholami *et al.* where the size of NPs slightly bigger (about 10 nm), this increase in hydrodynamic size leads to higher liver and spleen uptakes [30]. This exceptional characteristic of these NPs is due to their size and coating. Previous studies confirmed that dextran-coated particles with the size range between 60 to 80 nm were rapidly cleared from the blood and accumulated in the RES [21, 23, 30-34]. They got similar results in terms of short blood half-life and high RES uptakes and suggested that using theranostics radioisotopes such as ^{177}Lu or ^{153}Sm would be better for RES detection and therapeutic purposes. We could deliver high quantities of dose to the targeted organs (liver and spleen) with this brilliant phenomenon and since the tracer cleared so fast from blood the other organs (except RES) uptakes were negligible, although further study which involves medical internal radiation dosimetry (MIRD) of the radio compound is still needed to predict human absorbed dose based on the biodistribution data in rodents [10, 11]. Weissleder *et al.* in *1988* showed that the SPION with 80 nm mean size commercially available as AMI-25 after 1 hour post i.v. injection in rats more than 82% and 6% of injected dose were accumulated in liver and spleen, respectively [35]. While in our study, more than 66% and 18% of administrated dose were taken up by the liver and spleen, respectively. In agreement to Weissleder *et al.* the no brain uptakes seen in brain which shows that the NPs cannot pass through the blood brain barrier (BBB).

Table 1 represented the decay-corrected biodistribution data of ^{111}In-DTPA-SPION at various time points after intravenous injection through the mice's tail vein. As can be seen while the radiolabeled SPIONs were cleared rapidly from the blood, they accumulated in the liver and spleen. From the first minutes post injection the blood activity decreased rapidly. Thus at 30 minutes post injection just 1% ID/g still remained in the blood while the liver had taken up about 70% ID/g. The spleen uptake trend is similar to that of the liver but/though the uptake amounts were less than one third at each time point. At 30 minutes post injection both liver and spleen reached their maximum uptakes (69.82 and 21.39 for the liver and spleen, respectively) while the other organ activities were negligible except for kidneys and urine which showed about 2% of ID/g. This pattern is similar to those observed in our previous studies and other studies, and confirms that, due to their large size, these nanoparticles (i.e.:80 nm) cannot behave as a blood pool agent as they are absorbed by the liver and spleen.

As represented in table 1 after 30 minutes post injection more than 84% of injected activities were taken up by the liver and spleen (about 64% and 20%, respectively).

Due to impressive amount of cumulative activity in the RES, the effective absorbed dose in these two organs were so high compare to normal human diagnostic nuclear medicine studies. As can be calculated from table 1, the spleen/blood and liver/blood uptake ratios would be rapidly raised by the time increased. For instance; uptakes ratios after 30 min post injection would be more than 19 and 63, respectively for spleen/blood and liver/blood. These ratios rose dramatically after 6 hours post injection into 61 and 223, correspondingly. Further studies still needed to calculate the internal dose and safety of this radiotracer [36, 37].

[Downloaded from ijrr.com on 2025-07-12]

[DOI: 10.18869/acadpub.ijrr.18.3.511]

CONCLUSIONS

The biodistribution of ^{111}In-DTPA-SPION in mice showed spectacular uptake in the reticuloendothelial system (RES) and the blood clearance was so fast. In conclusion, due to magnificent uptakes of this radiotracer in the liver and spleen, its stability and their fast clearance from other tissues, especially in blood, it is suggested that this radiotracer would be suitable for RES theranostics purposes.

Conflicts of interest: *Declared none.*

REFERENCES

1. Najafian N, Shanehsazzadeh S, Hajesmaeelzadeh F, Lahooti A, Gruettner C, Oghabian MA (2015) Effect of Functional Group and Surface Charge of PEG and Dextran-Coated USPIO as a Contrast Agent in MRI on Relaxivity Constant. *Appl Magn Reson,* ***46:*** *685-92.*
2. Shanehsazzadeh S, Lahooti A, Hajipour MJ, Ghavami M, Azhdarzadeh M (2015) External magnetic fields affect the biological impacts of superparamagnetic iron nanoparticles. *Colloids Surf B Biointerfaces,* ***136:*** *1107-12.*
3. Oghabian MA, Gharehaghaji N, Masoudi A, Shanehsazzadeh S, Ahmadi R, Majidi RF, *et al.* (2013) Effect of coating materials on lymph nodes detection using magnetite nanoparticles. *Adv Sci Eng Med,* ***5:*** *37-45.*
4. Laurent S, Saei AA, Behzadi S, Panahifar A, Mahmoudi M (2014) Superparamagnetic iron oxide nanoparticles for delivery of therapeutic agents: opportunities and challenges. *Expert Opin Drug Deliv,* ***11:*** *1449-70.*
5. Mousavie Anijdan SH, Shirazi A, Mahdavi SR, Ezzati A, Mofid B, Khoei S, *et al.* (2012) Megavoltage dose enhancement of gold nanoparticles for different geometric set-ups: Measurements and Monte Carlo simulation. *Int J Radiat Res,* ***10(3):*** *183-6.*
6. Shanehsazzadeh S, Oghabian MA, Allen BJ, Amanlou M, Masoudi A, Johari Daha F (2013) Evaluating the effect of ultrasmall superparamagnetic iron oxide nanoparticles for a long-term magnetic cell labeling. *J Med Phys,* ***38:*** *34-40.*
7. Hajesmaeelzadeh F, Shanehsazzadeh S, Grüttner C, Johari Daha F, Oghabian MA (2016) Effect of coating thickness of iron oxide nanoparticles on their relaxivity in the MRI. *Iran J Basic Med Sci,* ***19:*** *166-71.*
8. Lahooti A, Sarkar S, Laurent S, Shanehsazzadeh S (2016) Dual nano-sized contrast agents in PET/MRI: a systematic review. *Contrast Media Mol Imaging,* ***11:*** *428-47.*
9. Lederer CM, Hollander JM, Perlman I (1967) *Table of isotopes. John Wiley & Sons Inc.*
10. Fazaeli Y, Shanehsazzadeh S, Lahooti A, Feizi S, Jalilian AR (2016) Preclinical dosimetric estimation of [111In] 5, 10, 15, 20-tetra phenyl porphyrin complex as a possible imaging/PDT agent. *Radiochim Acta* ***104:*** *327–36.*
11. Lahooti A, Shanehsazzadeh S, Jalilian AR, Tavakoli MB (2013) Assessment of effective absorbed dose of 111In-DTPA-Buserelin in human on the basis of biodistribution rat data. *Radiat Prot Dosim,* ***154:*** *1-8.*
12. Jalilian AR, Sardari D, Kia L, Rowshanfarzad P, Garousi J, Akhlaghi M, *et al.* (2008) Preparation, quality control and biodistribution studies of two [111In]-rituximab immunoconjugates. *Scientia Pharmaceutica,* ***76(2):*** *151-70.*
13. National Institutes of Health (1985) Guide for the care and use of laboratory animals. *NIH Publication, 85-123*.
14. Omid H, Oghabian MA, Ahmadi R, Shahbazi N, Hosseini HR, Shanehsazzadeh S, *et al.* (2014) Synthesizing and staining manganese oxide nanoparticles for cytotoxicity and cellular uptake investigation. *Biochim Biophys Acta,* ***1840(1):*** *428-33.*
15. Hatamie S, Ahadian MM, Ghiass MA, Iraji Zad A, Saber R, Parseh B, *et al.* (2016) Graphene/cobalt nanocarrier for hyperthermia therapy and MRI diagnosis. *Colloids Surf B Biointerfaces,* ***146:*** *271-9*.
16. Jahanbakhsh R, Atyabi F, Shanehsazzadeh S, Sobhani Z, Adeli M, Dinarvand R (2013) Modified Gadonanotubes as a promising novel MRI contrasting agent. *Daru,* ***21:*** *53-62.*
17. Sahnehszzadeh S and Jalilian A (2009) Development of [67ga]-Dtpa-Gonadorelin in Normal Rats. *J Label Compd Rad,* ***52:*** *S326*.
18. Jalilian AR, Shanehsazzadeh S, Akhlaghi M, Garousi J, Rajabifar S, Tavakoli M (2008) Preparation and biodistribution of [67Ga]-DTPA-gonadorelin in normal rats. *J Radioanal Nucl Ch,* ***278:*** *123-9*.
19. Shanehsazzadeh S, Oghabian MA, Lahooti A, Abdollahi M, Haeri SA, Amanlou M *et al.* (2013) Estimated background doses of [67Ga]-DTPA-USPIO in normal Balb/c mice as a potential therapeutic agent for liver and spleen cancers. *Nucl Med Commun,* ***34:*** *915-25.*
20. Jalilian AR, Shanehsazzadeh S, Akhlaghi M, Kamalidehghan M, Moradkhani S (2010) Development of [111In]-DTPA-buserelin for GnRH receptor studies. *Radiochim Acta,* ***98:*** *113-9.*
21. Nosrati S, Shanehsazzadeh S, Yousefnia H, Gholami A, Grüttner C, Jalilian AR, *et al.* (2016) Biodistribution evaluation of 166Ho–DTPA–SPION in normal rats. *J Radioanal Nucl Ch,* ***307:*** *1559-66.*
22. Jalilian AR, Shanesazzadeh S, Rowshanfarzad P, Bolourinovin F, Majdabadi A (2008) Biodistribution study of [61 Cu] pyruvaldehyde-bis (N-4-methylthiosemicarbazone) in normal rats as a PET tracer. *Nucl Sci Tech,* ***19:*** *159-64.*
23. Lahooti A, Sarkar S, Rad HS, Gholami A, Nosrati S, Muller RN, *et al.* (2017) PEGylated superparamagnetic iron oxide nanoparticles labeled with 68Ga as a PET/MRI contrast agent: a biodistribution study. *J Radioanal Nucl Ch,* ***311:*** *769-774.*
24. Shanehsazzadeh S, Lahooti A, Shirmardi SP, Erfani M (2015) Comparison of estimated human effective dose of

[Downloaded from ijrr.com on 2025-07-12]

[DOI: 10.18869/acadpub.ijrr.18.3.511]

67Ga-and 99mTc-labeled bombesin based on distribution data in mice. *J Radioanal Nucl Ch,* ***305:*** *513-520.*

25. Zolghadri S, Jalilian AR, Naseri Z, Yousefnia H, Bahrami-Samani A, Ghannadi-Maragheh M, *et al.* (2013) Production, Quality Control and Biological Evaluation of 166Ho-PDTMP as a Possible Bone Palliation Agent. *Iran J Basic Med Sci,* ***16:*** *719-725.*
26. Jalilian A, Shanehsazzadeh S, Akhlaghi M, Garoosi J, Rajabifar S, Tavakoli M (2008) Preparation and evaluation of [67Ga]-DTPA-β-1–24-corticotrophin in normal rats. *Radiochim Acta,* ***96:*** *435-9.*
27. Shanehsazzadeh S, Lahooti A, Sadeghi HR, Jalilian AR (2011) Estimation of human effective absorbed dose of 67Ga-cDTPA-gonadorelin based on biodistribution rat data. *Nucl Med Commun,* ***32:*** *37-43.*
28. Shanehsazzadeh S, Yousefnia H, Jalilian AR, Zolghadri S, Lahooti A (2015) Estimated human absorbed dose for 68Ga-ECC based on mice data: comparison with 67Ga-ECC. *Ann Nucl Med,* ***29:*** *475-481.*
29. Shanehsazzadeh S, Yousefnia H, Lahooti A, Zolghadri S, Jalilian AR, Afarideh H (2015) Assessment of human effective absorbed dose of 67 Ga-ECC based on biodistribution rat data. *Ann Nucl Med,* ***29:*** *118-24.*
30. Gholami A and Mousavi Anijdan SH (2016) Development of 153Sm-DTPA-SPION as a theranostic dual contrast agents in SPECT/MRI. *Iran J Basic Med Sci,* ***19:*** *1056-62.*
31. Shanehsazzadeh S, Gruettner C, Lahooti A, Mahmoudi M, Allen BJ, Ghavami M*, et al.* (2015) Monoclonal antibody conjugated magnetic nanoparticles could target MUC-1-positive cells in vitro but not *in-vivo*. *Contrast Media Mol Imaging,* ***10:*** *225-36.*
32. Lahooti A, Shanehsazzadeh S, Oghabian MA, Allen BJ (2013) Assessment of human effective absorbed dose of Tc-99m-USPIO based on biodistribution rat data. *J Label Compd Rad* ***56:*** *S258.*
33. Haeri G, Rajabi HO, Akhlaghpoor S (2014) SPIO-Annexin V, a potential probe for MRI detection of radiation induced apoptosis. *Int J Radiat Res,* ***12(3):*** *217-222*.
34. Shanehsazzadeh S and Lahooti A (2014) Biodistribution of 80 nm iron oxide nanoparticles labeled with 99mTc in Balb/c mice. *Nucl Med Biol,* ***41:*** *625.*
35. Weissleder R, Stark DD, Engelstad BL, Bacon BR, Compton CC, White DL*, et al.* (1989) Superparamagnetic iron oxide: pharmacokinetics and toxicity. *Am J Roentgenol,* ***152:*** *167-73.*
36. Shanehsazzadeh S, Lahooti A, Yousefnia H, Geramifar P, Jalilian AR (2015) Comparison of estimated human dose of 68Ga-MAA with 99mTc-MAA based on rat data. *Ann Nucl Med,* ***29:*** *745-53.*
37. Sadeghzadeh M, Shanehsazzadeh S, Lahooti A (2015) Assessment of the effective absorbed dose of 4-benzyl-1-(3-[125I]-iodobenzylsulfonyl)piperidine in humans on the basis of biodistribution data of rats. *Nucl Med Commun* ***36:*** *90-4.*

[Downloaded from ijrr.com on 2025-07-12]

[DOI: 10.18869/acadpub.ijrr.18.3.511]

[Downloaded from ijrr.com on 2025-07-12]

[DOI: 10.18869/acadpub.ijrr.18.3.511]